Evaluation of ALOS/PALSAR L-Band Data for the Estimation of *Eucalyptus* Plantations Aboveground Biomass in Brazil

Nicolas Baghdadi, Guerric Le Maire, Jean-Stéphane Bailly, Kenji Osé, Yann Nouvellon, Mehrez Zribi, Cristiane Lemos, and Rodrigo Hakamada

***Abstract*—The Phased Array L-band Synthetic Aperture Radar (PALSAR-1) has provided very useful images dataset for several applications such as forestry. L-Band radar measurements have been widely used but with somewhat contradictory conclusions on the potential of this radar wavelength to estimate the aboveground biomass (AGB). The first objective of this study was to analyze the L-band SAR backscatter sensitivity to forest biomass for *Eucalyptus* plantations. The results showed that the radar signal is highly dependent on biomass only for values lower than 50 t/ha, which corresponds to plantations of approximately 3 years of age. Next, random forest (RF) regressions were performed to evaluate the potential of PALSAR data to predict the *Eucalyptus* biomass. Regressions were constructed to link the biomass to both radar signal and age of plantations. Results showed that the age was the variable that best explained the biomass followed by the PALSAR HV polarized signal. For biomasses lower than 50 t/ha, HV signal and plantation age were found to have the same level of importance in predicting biomass. For biomasses higher than 50 t/ha, plantation age was the main variable in the RF models. The use of PALSAR signal alone did not correctly predict the biomass of *Eucalyptus* plantations [R^2 lower than 0.5 and root-mean-squared error (RMSE) higher than 46.7 t/ha]. The use of plantation age in addition to the PALSAR signal improved slightly the prediction results (R^2 increased from 0.88 to 0.92 and RMSE decreased from 22.7 to 18.9 t/ha). PALSAR imagery does not allow a direct estimation of planting date of *Eucalyptus* stands but can follow efficiently the occurrence of clear-cuts if images are acquired sequentially, therefore allowing a rough estimate of the following plantation date because a stand of *Eucalyptus* is generally replanted 2–4 months after cutting. With a time series of radar images, it could be, therefore, possible to estimate the plantation age, and therefore improving the estimates of plantation biomass.**

Manuscript received December 17, 2013; revised April 23, 2014; accepted August 27, 2014. This work was supported by the French Space Study Center (CNES, DAR 2014 TOSCA).

N. Baghdadi and K. Osé are with the IRSTEA, UMR TETIS, 34093 Montpellier Cedex 5, France (e-mail: nicolas.baghdadi@teledetection.fr; kenji.ose@teledetection.fr).

G. Le Maire and Y. Nouvellon are with the CIRAD, UMR Eco&Sols, 34060 Montpellier, France (e-mail: guerric.le_maire@cirad.fr; yann.nouvellon@cirad.fr).

J.-S. Bailly is with the AgroParisTech, UMR TETIS–LISAH, 34093 Montpellier Cedex 5, France (e-mail: jean-stephane.bailly@teledetection.fr).

M. Zribi is with the CESBIO, 31401 Toulouse Cedex 9, France (e-mail: Mehrez.Zribi@ird.fr).

C. Lemos and R. Hakamada are with the International Paper do Brasil, São Paulo, Brazil (e-mail: Cristiane.Lemos@ipaperbr.com; Rodrigo.Hakamada@ipaperbr.com).

Color versions of one or more of the figures in this paper are available online at http://ieeexplore.ieee.org.

Digital Object Identifier 10.1109/JSTARS.2014.2353661

***Index Terms*—Aboveground biomass (AGB), Brazil, *Eucalyptus*, fast-growing plantations, L-band ALOS/PALSAR, short-rotation plantations.**

I. Introduction

FORESTS aboveground biomass (AGB) represents a major biospheric carbon pool [1]. Changes in this pool through deforestation/reforestation activities, forest degradation, or regrowth lead to large CO_2 fluxes (emissions and uptake) that strongly influence the global C cycle and climate system [1], [2]. Forest biomass is also an important economic product, providing materials and energy for humans, and its spatial distribution influences some important ecosystem services such as conservation of biodiversity [3]. For all these reasons and also for forest management and the implementation of REDD+ mechanisms, accurate and effective observation systems are required to map and monitor forest AGB stocks [4], [5]. Satellite-based estimation of carbon biomass is a promising solution in terms of 1) cost- and time-effectiveness compared to large-scale field inventories and 2) spatial coverage and temporal repetitivity.

From the last two decades, a number of studies have examined the dependence of microwave backscatter on total AGB using airborne and spaceborne Synthetic Aperture Radar (SAR). According to some reports focused on the potential of multifrequency (C-, L-, and P-bands) and multipolarization data, the longer wavelengths (L- and P-bands) at a single polarization are sensitive to variations in AGB up to a certain biomass level at which the radar signal saturates [6]–[15]. However, only L-band SAR is currently onboard satellites such as the Phased Array L-band Synthetic Aperture Radar (PALSAR)/Advanced Land Observing Satellite (ALOS). Spaceborne P-band is not yet available.

Statistical analyses performed to evaluate the correlation between backscattering coefficient (σ^0) and AGB use mainly polynomial, logarithmic, or sigmoid functions. For L-band, the dynamic range of the cross-polarized HV response is often larger than copolarized HH or VV channels [6], [7], [16], [20]. Previous studies have shown that the most suitable SAR incidence angle in biomass retrieval is in the range 30°–45° [17]–[19]. Observations at lower incidence angles (20°–30°) will allow higher penetration into the forest canopy and potentially larger sensitivity to biomass. However, at these incidence angles, the contribution of the ground increases, in particular for low biomasses, hence increasing the error on the biomass

estimates. The level of signal saturation occurs when AGB exceeds approximately 60–100 t/ha. On the L-band SAR, various forest types have been investigated. Le Toan *et al.* [16], Wu *et al.* [21], and Dobson *et al.* [8] reported in coniferous forests (maritime pine and loblolly pine) a backscatter saturation AGB levels of 100 t/ha. According to Imhoff [22], the practical saturation thresholds occur before the regression maxima due to the large residuals near the point of inflection and beyond it and the biomass saturation levels would be rather close to 40 t/ha. Rignot *et al.* [6], Ranson and Sun [9], and Sandberg *et al.* [23] observed in boreal forests (conifer and deciduous trees) that the backscatter intensity increases with biomass up to 100–150 t/ha. In tropical forests (broadleaf evergreen trees), Luckman *et al.* [7], [24], who has investigated regenerating forests in the Central Amazon basin, reported a saturation point around 60 t/ha. The results presented in that study focused on monospecific and even-aged forests with a relatively flat topography. Some studies applied on mixed-species forests without species-discrimination obtained similar saturation levels.

As argued by Woodhouse *et al.* [25], the radar backscatter is not a "direct measure" of forest biomass. It may be strongly affected by the forest structure [10], [11], [26]–[28] as well as its spatial variability [12]. Hence, the backscatter saturation depends on stand characteristics related to biomass such as the size, density, and spatial distribution of the stems, branches, and leaves.

Regardless of slope and surface roughness characteristics, the backscatter signal may also be affected by surface and vegetation moisture conditions. Few studies investigated this issue and there is no consensus among scientists [20], [29]. Nevertheless, Lucas *et al.* [20] demonstrated the greater sensitivity of L-band HH to surface moisture. While the forest AGB at backscatter saturation level remains similar for L-band HV under conditions of relative maximum surface moisture, it is reduced for L-band HH. An analysis of the radar backscatter from *Eucalyptus* plantations in Congo showed that the L-HH signal was strongly influenced by the ground surface [29]. This direct contribution of the ground surface depended mainly on the soil moisture and roughness.

Luckman *et al.* [24] observed a variation in dynamic range and saturation in backscatter (L-band HH and JERS-1) within seasonal cycle. For Harrell *et al.* [13], the presence of wet soils introduces an additional source of variability that increases the root-mean-squared error (RMSE) of the predictive biomass equations. Of these studies, the dry season was found to be the most suitable acquisition period for biomass retrieval purpose.

More complex approaches were presented in studies dealing with the use of SAR data for biomass estimation [30], [31]: the synergistic use of multiple-channel radar imagery (e.g., the use of HV backscattering from two channels, a longer wavelength [P- or L-band] and a shorter wavelength [C-band or X-band]) [9], [32], the use of different polarizations [6], [14], and the use of multiple-step approaches [11], [13], [33] that take into account separate layers of forest and finally determine total AGB. Those methods would allow higher biomass estimation (up to 200–600 t/ha according to forest stands) with a better precision than correlations between total biomass and radar backscatter from a single frequency/polarization system.

Whatever the method applied, it is necessary to stratify the forests into categories following their characteristics (structure, species, and moisture conditions) before applying SAR backscatter-based biomass estimation models.

The objective of this study was to assess the potential of PALSAR L-band data for the estimation of the *Eucalyptus* plantation AGB in Brazil. Recently, Gama *et al.* [34] used airborne interferometric and polarimetric SAR data in X and P bands to estimate *Eucalyptus* biomass in the southeast region of Brazil. A *Eucalyptus* biomass model was obtained with a prediction error of around 10% on the retrieval of *Eucalyptus* biomass. It used the canopy scattering index calculated from the P band backscatter magnitude data and the interferometric height defined by the difference between interferometric digital elevation model in X and P bands. Le Maire *et al.* [35] proposed an efficient method based on the use of MODIS NDVI time-series and bioclimatic data and soil type for estimating *Eucalyptus* plantation biomass: the age of the plantation and the NDVI integrated over the first 2 years of plantation growth were used to estimate wood biomass with an accuracy of about $25\ \mathrm{m}^3/\mathrm{ha}$, corresponding to about 13 t/ha. Baghdadi *et al.* [36] tested the use of ICESat/GLAS satellite LiDAR data for estimating AGB in the same *Eucalyptus* plantations. First, the height of planted *Eucalyptus* forest stands was estimated from GLAS waveform metrics. Next, the AGB was estimated using a power law model between the biomass and the GLAS-derived height, giving a final accuracy of 16.1 t/ha for biomass values up to 170 t/ha.

In this study, the random forest (RF) regression method was used to assess the possibility of estimating accurately *Eucalyptus* stand biomass from the radar signal only or from the radar signal plus the plantation age. A description of study area, SAR images, and in situ measurements is given in Section II, followed by the sensitivity analysis of PALSAR signal to AGB. The potential of PALSAR images for the detection of plantation harvest is discussed in section III. Finally, the results obtained for the estimation of the biomass using PALSAR images and the RF method are presented and discussed in Section IV.

II. Datasets Description

A. Study Area

The study area was located in the state of São Paulo, Brazil, ranging from $46°49'$ to $48^deg10'$ longitude West and from $20°30'$ to $22°34'$ latitude South (Fig. 1). The study is focused on industrial fast-growing *Eucalyptus* plantations managed to produce pulpwood for paper production by the International Paper do Brasil company. They were planted with seedlings or clones of *E. grandis* (W. Hill ex Maiden) $\times$ *E. urophylla* (S.T. Blake) hybrids, arranged in rows at a density of approximately 1300 t/ha. Tree mortality after planting is very low (less than 7%; [37]). They are harvested (plantation clear-cutting) every 6–7 years. The annual increment varied according to the growth stage, soil type management practices (clone and fertilization), and climatic conditions but was generally higher than $30\ \mathrm{m}^3$/ha/year, sometimes reaching values as high as $60\ \mathrm{m}^3$/ha/year, thus leading to harvested volume

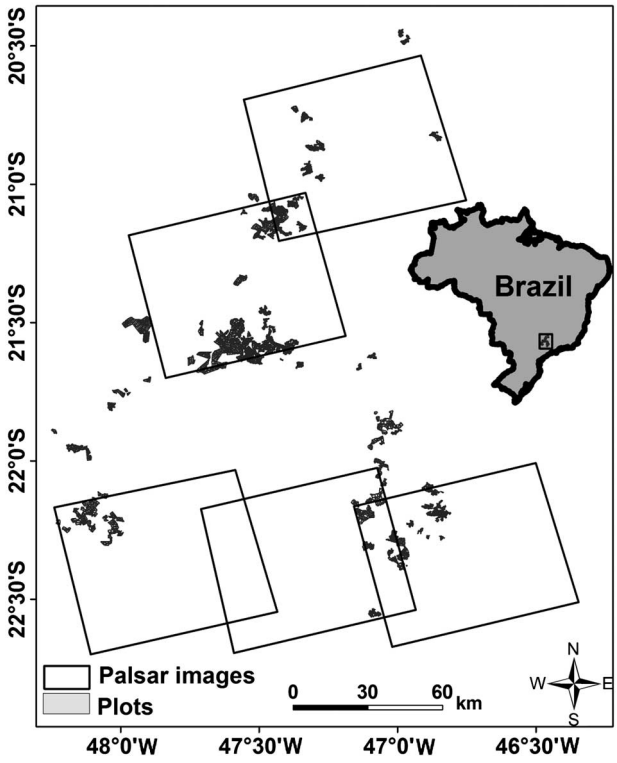

Fig. 1. Study site, *Eucalyptus* stands, and the coverage of PALSAR images.

of $250-300$ m^3/ha. These plantations were managed locally by stand units of variable area ($\sim$50 ha on average for studied stands). Management practices were uniform within each stand (e.g., harvesting and weeding dates, genetic material, soil preparation, and fertilization). Chemical weeding was carried out during the first 2 years after planting, resulting in a very sparse understory and herbaceous strata in these plantations. The stands were rather simply structured with a crown layer of 3–10 m in width above a dense "trunk layer" ranging from 0 (in the first months) up to more than 20 m in height with very few understories (Fig. 2). Branches biomass is almost constant during the plantation growth, with approximately 2 t/ha of living branches and 2 t/ha of dead branches. It can represent a significant amount of the total carbon content of the stand at the beginning of the rotation ($<$1 year), but at the end of the rotation, it account for less than 10% [38]. Branches are generally thin and oriented upward.

In the study area, the stands were established in a low-to-moderate topographic relief (slope under 7°).

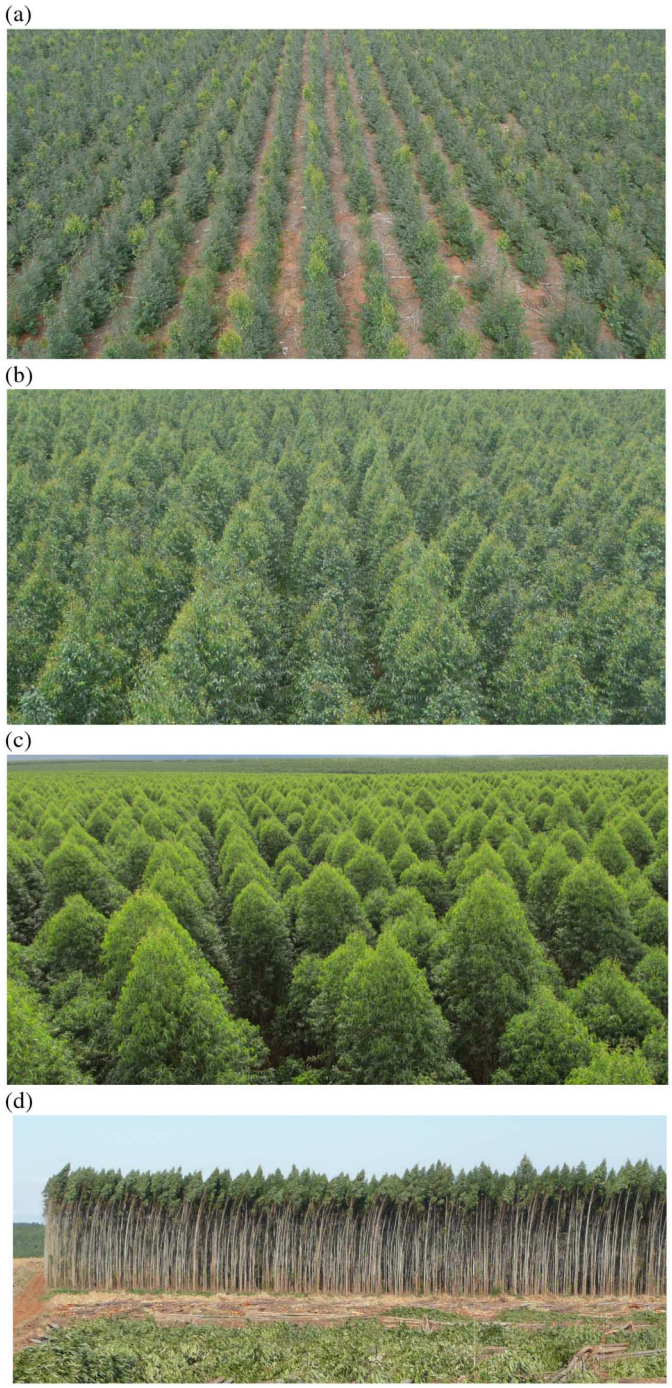

Fig. 2. Photos illustrating the *Eucalyptus* plantations at different ages: (a) 1 year; (b) 2 years; (c) 4 years; (d) during harvest (7 years).

B. ALOS/PALSAR Data

Twelve radar images acquired by the ALOS/PALSAR were used in this study (Table I). These images were acquired between July 2007 and August 2009 with dual polarization (HH and HV), incidence angles of 34.3°, and 12.5 m $\times$ 12.5 m pixel size. Radiometric calibration of PALSAR images were performed for obtaining the backscattering coefficients (σ°).

Before calculating the mean backscattering coefficient of each documented *Eucalyptus* stand, the radiometric quality of calibrated PALSAR images was analyzed using several homogeneous and dense stands of natural forests. Fig. 3 shows that the mean backscattering coefficient on these areas of interest is similar for all PALSAR images with -8.0 dB (± 0.7 dB) in HH polarization and -12.6 dB (± 0.6 dB) in HV polarization. However, an important decrease in the radar signal (several decibels) was observed on *Eucalyptus* stands for the two images acquired at the end of dry season (September 20 and October 19, 2007). The dry season effect may result from the partial shedding of *Eucalyptus* foliage (decrease in leaf area index) during drought, as observed on Landsat NDVI time series

TABLE I
CHARACTERISTICS OF PALSAR IMAGES

Date 2007 (dd/mm)	19/07; 20/09; 19/10
Date 2008 (dd/mm)	07/05; 05/06; 07/08; 24/08; 05/09 (2 images); 22/09
Date 2009 (dd/mm)	24/07; 10/08

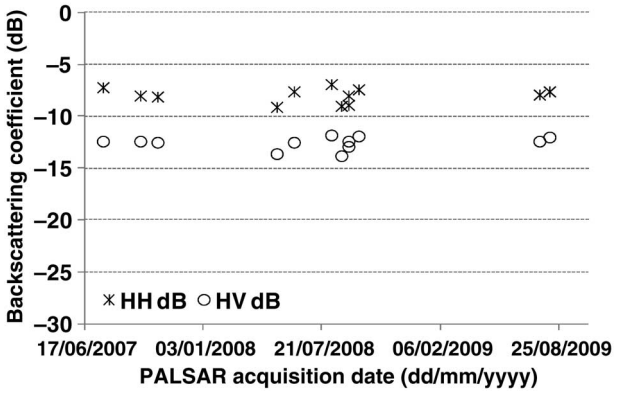

Fig. 3. Mean backscattering coefficient on stands of natural forests for the 12 PALSAR images used in this study.

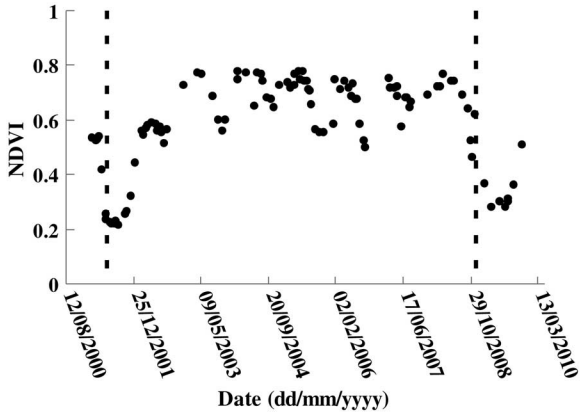

Fig. 4. Landsat NDVI time-series of a given *Eucalyptus* stand. Dashed line indicates the planting date.

(Fig. 4; Le Maire *et al.* [39]), and from lower soil surface humidity. These two images were removed of the following study.

C. In Situ Measurements

A total of 695 *Eucalyptus* stands were used, corresponding to the stands of International Paper do Brazil covered by our PALSAR images where inventory data were available. Permanent inventory plots had an area of approximately $400-600$ m^2 and were systematically distributed throughout the stand with a density of one plot per 12 ha. They included 30–100 trees (average of 58 trees). During a *Eucalyptus* rotation, three field inventories were generally carried out in every field plots (at age of 2 years, 4 years, and before harvesting). During a field inventory, the diameter at breast height (DBH, 1.3 m above the ground) of each tree in the inventory plot, the height of a central subsample of 10 trees, and the height of the 10% of largest DBH (dominant trees) were measured. The mean height of the 10% of the largest trees defined the dominant

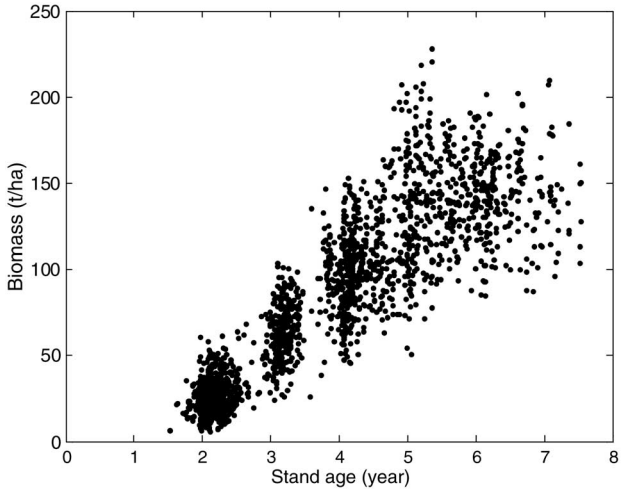

Fig. 5. *Eucalyptus* plantation biomass in function of stand age.

height of the plot (H_{dom}). The H_{dom}, basal area, and age at the inventory date were then used in a company-calibrated volume equation, specific to the genetic material, to estimate the plot stem volume (wood and bark of the merchantable part of the stem that has a diameter of more than 2 cm). Trunk biomass was then estimated from the trunk volume using age-dependent estimates of wood biomass density (see [40] for more details). Plot-scale biomass was then averaged to get stand-scale estimates, for each inventory date. Note that branches and leaves biomass represent only a small percentage of the trunk biomass after the first year of the rotation [38].

As the dates of the ground measurements were different from the PALSAR acquisition dates, biomass for the PALSAR acquisition dates were estimated using linear interpolations of the inventory plot measurements between the two dates either side of each PALSAR acquisition date, as was done in Baghdadi *et al.* [36]. This simple linear interpolation gave fairly good estimates since forest inventories were regularly carried out. These estimates of biomass gave a large dataset of 1255 single biomass-PALSAR pairs of values for testing the potential of PALSAR data to estimate the AGB.

Fig. 5 shows that the *Eucalyptus* stand biomass increases almost linearly with the stand age after 2 years old, but with a high-scattering hiding, the tendency for individual stands to have lower growth rates before 2 years old and after 5 years old. This correlation between age and biomass is at the basis of the method applied further in this study.

III. METHODOLOGY

This study will analyze first the sensitivity of PALSAR L-band SAR signal on the AGB of *Eucalyptus* plantations. As shown in the literature, the estimate of the biomass is usually possible with SAR signal for a certain range of biomass values, and beyond a given threshold, the radar signal becomes insensitive to the biomass [6]–[15]. The L-band radar signal saturation threshold is very different from one study to another due in particular to the characteristics of the vegetation (thresholds between 40 and 150 t/ha, e.g., [41]. This analysis of the

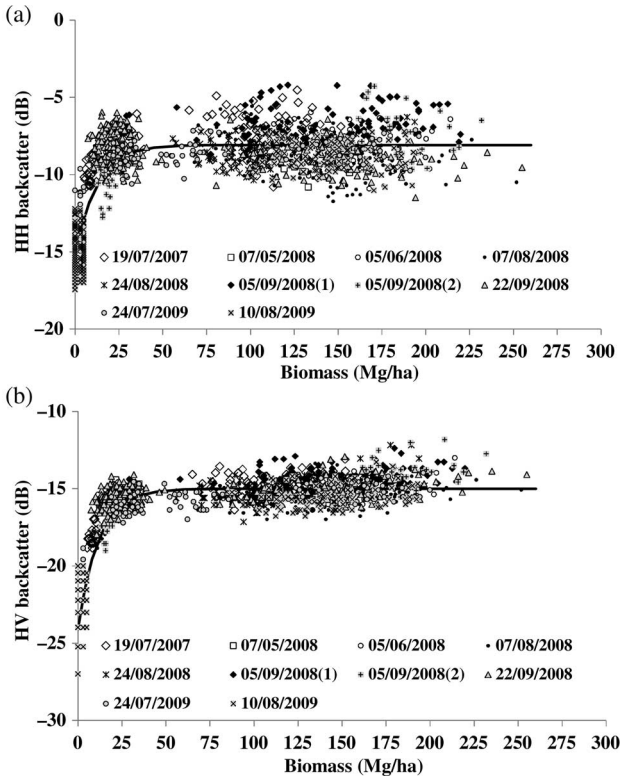

Fig. 6. Relationships between PALSAR signal and AGB: (a) HH polarization and (b) HV polarization.

radar signal on *Eucalyptus* stands will allow us to determine the range of biomass values for which the radar signal may be used alone to estimate biomass with acceptable accuracy. This PALSAR saturation threshold will be determined according to HH and HV polarizations.

The second part of this study analyzes the accuracy of AGB estimates obtained from the PALSAR signal alone, or from the PALSAR signal and the plantation age as an additional information. Then, the potential of PALSAR images for estimating the plantation age will be evaluated. Finally, nonlinear nonparametric regressions will be performed in order to estimate wood biomass as accurately as possible.

IV. PALSAR Behavior Analysis

The mean backscattering coefficient was computed for each reference stand and each polarization. Fig. 6 shows that the PALSAR signal increases with the AGB until a saturation threshold. For biomasses below 30–50 t/ha, the radar signal showed a high sensitivity to biomass values. After this threshold, the radar signal saturated. This threshold value of the biomass was relatively low when compared with the biomass of our *Eucalyptus* stands after 3 years of age. Results also showed that the HV polarization (σ°HV) produced better correlation ($R^2 = 0.85$) with the biomass than the HH polarization (σ°HH) ($R^2 = 0.71$). This better correlation between σ°HV and the biomass is mainly due to volume scattering that enhances the cross-polarization returns with the increase in biomass (e.g.,[14], [18], [27], [42], [43]).

The relationship between the PALSAR signal in HH polarization and biomass is noisier than in HV band. Mitchard *et al.* [28] also observed in HH high fluctuations for PALSAR data acquired in the wet season and low fluctuations for JERS data acquired during the dry season. They explained that the soil moisture effect during the wet season could be responsible for the observed high fluctuation in the radar signal at HH polarization as well as structural variation within a stand. Collins *et al.* [43] argued that σ°HV is less influenced by soil and vegetation moisture than σ°HH.

The scattering mechanisms contributing to the total backscatter depends on forest structure (characteristics of leaves, branches, and trunks). Several results of SAR modeling based on the simulation model of Karam [44] indicated that for *Mangrove* forests [45], [46], the return signal was mainly dominated in HV polarization by the volume scattering (crown layer: leaves and branches) for forests with high biomass values ($>30-50$ t/ha). For biomass values lower than 30–50 t/ha, the volume scattering and the interactions between the tree components and the ground contribute equally to L-HV. For the HH polarization, the total backscatter was dominated for biomasses lower than 200 t/ha by the interactions between the larger branches and trunks and also ground surface. At L-HH and biomass values higher than 200 t/ha, the volume scattering increased and the ground-vegetation interactions decreased with the increase in biomass.

According to the structure of *Eucalyptus forests*, we suppose that the contributing scattering mechanisms on the total backscatter are the same for both *Eucalyptus* and *Mangrove* forests with probably different magnitudes because *Mangrove* forests contains higher trees with bigger branches in comparison with *Eucalyptus* forests.

Imhoff [10], based on simulations using the Michigan Microwave Canopy Scattering model (MIMICS), showed that the effect of forest structure on SAR backscatter can be significant for forests with equivalent AGB. These results explain different biomass saturation limits observed in numerous studies, and the difficulty to propose a universal SAR biomass equation for Globe's forest.

The increase in radar backscatter (σ°) against AGB (B) followed a logarithmic or exponential behavior (e.g., [28], [47], [48]). The best fitting relationship between PALSAR signal and the biomass was found in using an exponential model

$$\sigma^\circ = \alpha + \beta(1 - e^{-\mu B}) \quad (1)$$

where σ° and B are expressed in dB and t/ha, respectively. The coefficients α, β, and μ were fitted using a least squares fitting method. For HH polarization, $\alpha = -15.36$, $\beta = 7.28$, and $\mu = 0.08$ with $R^2 = 0.71$. For HV, the following values were found: $\alpha = -24.11$, $\beta = 9.11$, and $\mu = 0.09$ with $R^2 = 0.88$.

Imhoff [22] analyzed the effect of forest structure on the radar signal for several forest stands (natural forest and plantations including *Eucalyptus*). He showed that the radar signal was mainly correlated with the surface area (SA) to vegetation volume (V) (i.e., biomass/wood density) ratio, rather than the volume only. For a same AGB, *Eucalyptus* stands have the lower values of SA/V ratio than natural forests. He showed that for both low and high biomasses (between 50 and 300 t/ha),

σ°HV in L-band decreased when SA/V decreased. For low values of biomass (50 t/ha), the decrease in σ°HV was about 3 dB when SA/V decreased from 617 m^{-1} (1-year-old regenerating tropical forest) to 90 m^{-1} (*Eucalyptus* plantations aged 5 years old and more). For high biomass (300 t/ha), σ°HV decreased by about 9 dB for a decrease in SA/V from 254 m^{-1} (tropical evergreen rain forest) to 84 m^{-1} (tropical evergreen and tropical deciduous plantations). In our data, the trunk SA/V values (under the realistic hypothesis that branches have a very low volume and surface compared with the trunk) are comprised between 100 m^{-1} at 2 years of age and 60 m^{-1} at 6 years of age; therefore, a rather low amplitude. This result explains the observed low dynamic of radar signal for our *Eucalyptus* stands (low SA/V) in comparison with other forest types where SA/V is generally higher.

V. Harvest Detection From PALSAR

In general, *Eucalyptus* stands are replanted 2–4 months after clear-cutting. Radar imagery does not allow to estimate directly the planting date but can provide an approximation of it through the accurate estimate of the clear-cut date if the temporal resolution of images is high. In this section, the opportunity to detect the clear-cuts using PALSAR images will be analyzed at HH and HV polarizations. This harvesting date retrieval is possible with optical satellite images [35], but radar images can be very effective in areas with dense cloud covers.

Fig. 7 shows that the PALSAR images are suitable to monitor the Eucalyptus harvest. The radar signal decreases after the clear-cut by about −7 dB in HV (decreases from −16 dB for mature *Eucalyptus* to −23 dB for recently harvested *Eucalyptus*) and −5.5 dB in HH (decreases from −10 dB for mature *Eucalyptus* to −15.5 dB after the cut) [Fig. 7(a) and (b), plot A]. The clear-cut remains easily detectable on PALSAR images for data acquired less than 1 year after the harvest, with 3 dB difference in radar signal between harvested plots and mature Eucalyptus plots [Fig. 7(c) and (d), plot B harvested in October 2006]. After 18 months, the difference in radar signal becomes negligible (<1 dB) [Fig. 7(c) and (d), plot B, June 2008].

VI. Biomass Estimation

RF models [49] were used to evaluate the potential of PALSAR data to predict the Eucalyptus biomass. This nonparametric ensemble learning technique, based on the vote ensemble of a forest of randomized regression trees, has been proved to outperform other regression techniques in forested biophysical parameters estimation from optical [35], [50], radar [51], or lidar data [52]. RF have tremendous analytical and operational flexibility, it can deal with problems of unbalanced and small-sized training datasets. Moreover, it is robust to overfitting [49], [53]. Several recent studies have demonstrated the utility of RF for the prediction of forest structure attributes [53].

The dataset was randomly divided into 90% training and 10% validation data samples (1130 and 125, respectively).

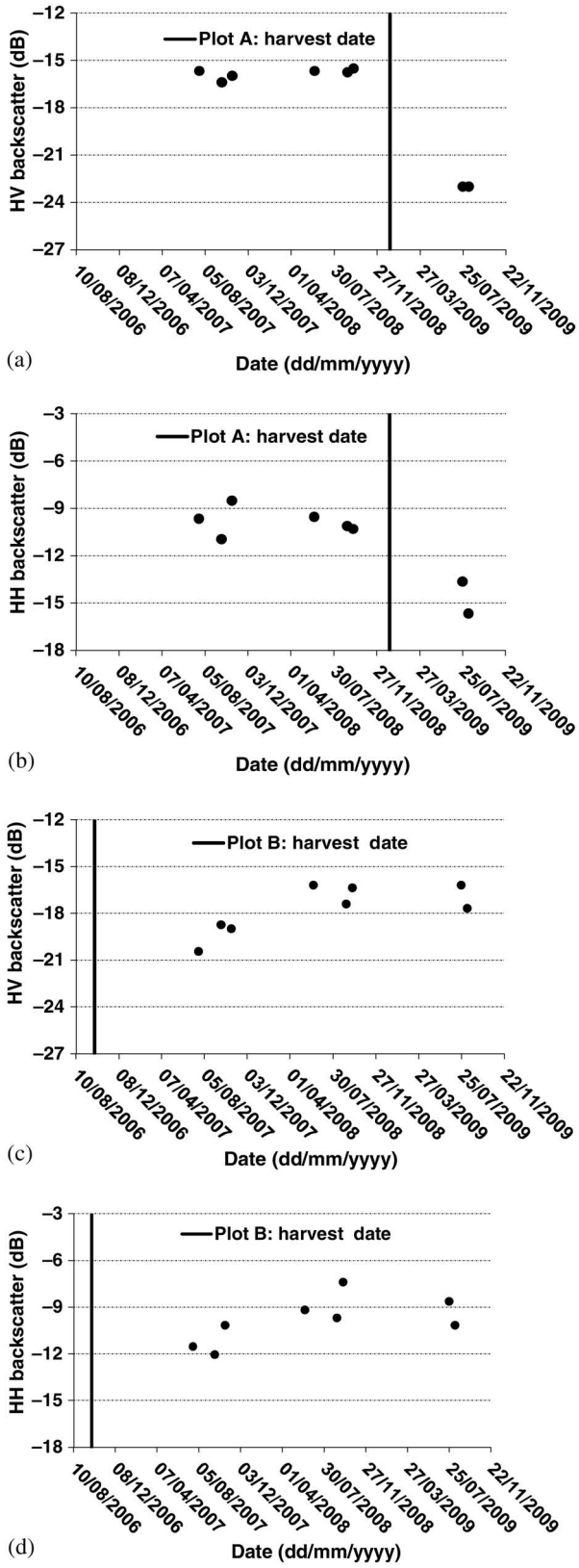

Fig. 7. Time sequences of PALSAR backscatter signal at HV and HH polarizations for two *Eucalyptus* reference plots (A and B). According to the inventories, plot A was harvested in January 2009 while plot A was harvested in October 2006.

TABLE II
ACCURACY ON THE ESTIMATION OF BIOMASS IN USING RF ALGORITHM AND DIFFERENT VARIABLES

Variables	R^2	RMSE (t/ha)
σ°HH	0.15	61.1
σ°HV	0.48	47.8
σ°HH ; σ°HV	0.50	46.7
Age of plantation	0.88	22.7
σ°HH ; Age	0.90	21.3
σ°HV ; Age	0.92	19.2
σ°HH ; σ°HV ; Age	0.92	18.9

The prediction error based on a 10-fold cross-validation was estimated for each configuration in order to validate the predictive performance of the RF.

Regressions were constructed to link the biomass to both radar signal and plantation age. Several configurations were tested and the performance of the RF algorithm on the PALSAR data was investigated using: 1) σ°HH alone; 2) σ°HV alone; 3) σ°HH and σ°HV; 4) age alone; 5) σ°HH and age; 6) σ°HV and age; and 7) σ°HH and σ°HV and age.

The performance of the RF regression for each studied configuration was analyzed from the comparison between measured and predicted biomasses, using the coefficient of determination R^2 and the RMSE. First, the relative importance of different variables used in the various RF models was investigated. Results showed that the plantation age was the variable that best explained the biomass followed by the PALSAR HV polarized signal. Better results were obtained with PALSAR signal in HV than in HH as was already seen from the exponential fit of (1).

The analyses of PALSAR signal according to biomass showed that the dynamic of the signal was very strong for biomasses lower than 50 t/ha (i.e., for plantation age <3 years) (Fig. 6). Thus, the importance of different variables (age, HV, and HH) in the models was analyzed separately for biomasses lower than 50 t/ha and higher than 50 t/ha. For biomasses lower than 50 t/ha, results showed that the HV signal and the age of plantation have the same level of importance in predicting the biomass and that the importance of HH signal is slightly lower. For biomasses higher than 50 t/ha, the age of plantation is the relevant variable.

The RF results are presented in Table II. They show that the use of PALSAR signal alone (σ°HH alone, or σ°HV alone, or σ°HH and σ°HV) does not correctly predict the biomass of Eucalyptus plantations (R^2 lower than 0.5 and RMSE higher than 46.7 t/ha). σ°HV was found more sensitive to forest biomass compared with σ°HH (R^2 and RMSE are, respectively, of 0.48 and 47.8 t/ha for σ°HV, and of 0.15 and 61.1 t/ha for σ°HH). From our results, the age of plantation has proved to be the most relevant variable in the prediction of the biomass that offered the best overall predictive accuracy ($R^2 = 0.88$ and $\mathrm{RMSE} = 22.7\mathrm{t/ha}$). Finally, the use of the plantation age in addition to the PALSAR signal (σ°) improves slightly the prediction results (R^2 increases from 0.88 to 0.92 and RMSE decreases from 22.7 to 18.9 t/ha).

RF regressions were also performed in using a threshold value on the plantation age (3 years) which corresponds to the saturation limit of the radar signal with the biomass. Regressions were constructed to link the biomass to both radar signal and plantation age, using separately stands with plantation age lower and higher than 3 years: 1) σ°HH and σ°HV and age <3 years and 2) σ°HH and σ°HV and age >3 years. Estimated biomass accuracy was 5.0 and 23.4 t/ha for plantation age lower and higher than 3 years, respectively. The higher accuracy until 3 years could be an opportunity to apply these results, using PALSAR as a tool to capture the quality of silviculture activities, once it affects the initial growth of the stand [54]. The overall accuracy ($\mathrm{RMSE} = 18.4\mathrm{t/ha}$) is close to the accuracy obtained by the regression without threshold on the plantation age ($\mathrm{RMSE} = 18.9\mathrm{t/ha}$).

Fig. 8 shows examples of comparisons between measured and predicted biomasses, obtained from a selection of variables in the RF algorithm. Without the use of the age of plantation, RF tended to over-estimate biomass below 50 t/ha and underestimate biomass above 50 t/ha [Fig. 8(a)]. Using plantation age in the regressions provided much better results [Fig. 8(b) and (c)].

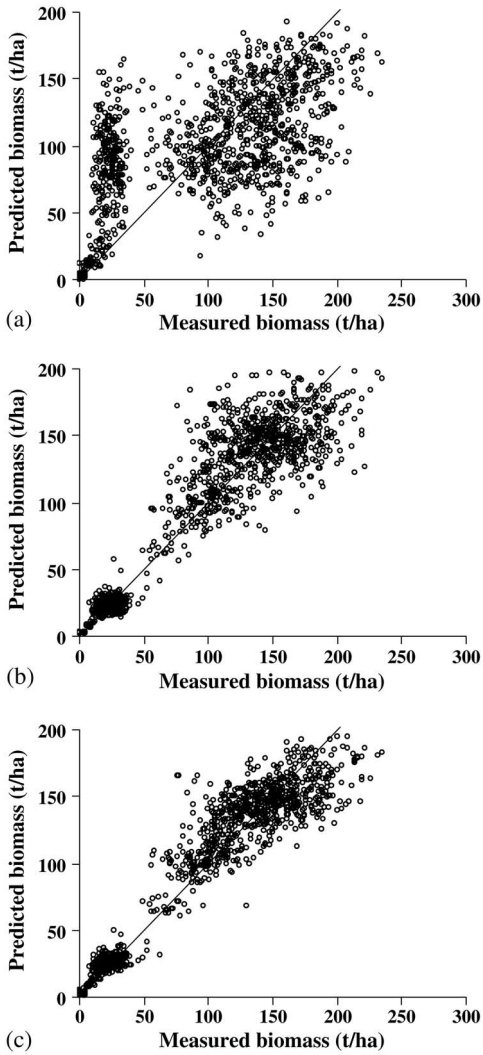

Fig. 8. Comparison of predicted and measured biomass using RF algorithm and three configurations: (a) σ°HH and σ°HV; (b) age of plantation; (c) σ°HH and σ°HV and age.

VII. Conclusion

This study aimed to examine the potential of L-band SAR images to estimate biomass in *Eucalyptus* plantations. RF regressions were performed and evaluated for biomass estimation. As in some previous studies, a rapid saturation of PALSAR signal with increasing biomass was observed (threshold of about 50 t/ha). Some other studies found a much higher threshold with saturation occurring for biomass levels of about 150–200 t/ha [27], [32], [43]. The large range of L-band saturation thresholds reported in the literature (i.e., from 30 to 200 t/ha) was mainly ascribed to the variability in vegetation structure across forest ecosystems [25].

Our results suggest that for fast-growing *Eucalyptus* plantations, it might be necessary to combine the backscattered signal with other data sources, such as the plantation age, that is accessible from SAR imagery itself, in order to obtain accurate biomass estimates, especially for high biomass levels. The overall accuracy for the RF regression using the plantation age and the PALSAR backscattered signals in HH and HV polarizations was 18.9 t/ha, a much better result than those obtained with regressions based only on the backscattered signals ($\mathrm{RMSE} = 46.7\ \mathrm{t/ha}$). Furthermore, for high biomass levels, the RF regression tended to underestimate the biomass.

With the upcoming launch of ALOS-2 sensor, the L-band radar data could be used to provide good estimates of the biomass of *Eucalyptus*. The probable arrival of BIOMASS P-band sensor (planned by the European Space Agency; [55]) should allow improved estimates of biomass with higher dynamic of the radar signal according to biomass (saturation of radar signal for biomass higher in P-band than in L-band).

Results of this study showed that the acquisition of SAR images in the same season is necessary for biomass estimation. Indeed, important differences in the radar signal were observed between images acquired in different seasons (water stress in the dry season), which makes the estimation of biomass inaccurate from SAR images acquired at different seasons.

Acknowledgment

The authors wish to thank the European Space Agency (ESA) and the Japan Aerospace Exploration Agency (JAXA) for the distribution of PALSAR/ALOS images (project AOALO 3610). The authors acknowledge International Paper do Brasil, and in particular J. M. Ferreira and S. Oliveira, for providing data and technical help. They also extend their thanks to C. Marsden (International Centre for Higher Education in Agricultural Sciences, SupAgro, Montpellier, France) for her participation in the inventory data preparation.

References

[1] Y. Pan *et al.*, "A large and persistent carbon sink in the world's forests," *Science*, vol. 333, no. 6045, pp. 988–993, 2011.

[2] R. A. Houghton *et al.*, "Carbon emissions from land use and land-cover change," *Biogeosciences*, vol. 9, pp. 5125–5142, 2012.

[3] T. Le Toan *et al.*, "The BIOMASS mission: Mapping global forest biomass to better understand the terrestrial carbon cycle," *Remote Sens. Environ.*, vol. 115, pp. 2850–2860, 2011.

[4] R. Birdsey Y. Pan, and R. A. Houghton, "Sustainable landscapes in a world of change: Tropical forests, land use and implementation of REDD+: Part I," *Carbon Manage.*, vol. 4, pp. 465–468, 2013.

[5] R. A. Houghton, "The emissions of carbon from deforestation and degradation in the tropics: Past trends and future potential," *Carbon Manage.*, vol. 4, pp. 539–546, 2013.

[6] E. Rignot, J. Way, C. Williams, and L. Viereck, "Radar estimates of aboveground biomass in boreal forests of interior Alaska," *IEEE Trans. Geosci. Remote Sens.*, vol. 32, no. 5, pp. 1117–1124, Sep. 1994.

[7] A. Luckman, J. Baker, T. M. Kuplich, C. da Costa Freitas Yanasse, and A. C. Frery, "A study of the relationship between radar backscatter and regenerating tropical forest biomass for spaceborne SAR instruments," *Remote Sens. Environ.*, vol. 60, pp. 1–13, 1997.

[8] M. C. Dobson *et al.*, "Dependence of radar backscatter on coniferous forest biomass," *IEEE Trans. Geosci. Remote Sens.*, vol. 30, no. 2, pp. 412–415, Mar. 1992.

[9] K. Ranson and G. Sun, "Mapping biomass of a northern forest using multifrequency SAR data," *IEEE Trans. Geosci. Remote Sens.*, vol. 32, no. 2, pp. 388–396, Mar. 1994.

[10] M. L. Imhoff, "Radar backscatter and biomass saturation: Ramifications for global biomass inventory," *IEEE Trans. Geosci. Remote Sens.*, vol. 33, no. 2, pp. 511–518, Mar. 1995.

[11] E. S. Kasischke, N. L. Christensen, and L. L. Bourgeau-Chavez, "Correlating radar backscatter with components of biomass in loblolly pine forests," *IEEE Trans. Geosci. Remote Sens.*, vol. 33, no. 3, pp. 643–659, May 1995.

[12] S. Saatchi, M. Marlier, R. L. Chazdon, D. B. Clark, and A. E. Russell, "Impact of spatial variability of tropical forest structure on radar estimation of aboveground biomass," *Remote Sens. Environ.*, vol. 115, pp. 2836–2849, 2011.

[13] P. A. Harrell, E. S. Kasischke, L. L. Bourgeau-Chavez, E. M. Haney, and N. L. Christensen, "Evaluation of approaches to estimating aboveground biomass in southern pine forests using SIR-C data," *Remote Sens. Environ.*, vol. 59, pp. 223–233, 1997.

[14] P. A. Harrell, L. L. Bourgeau-Chavez, E. S. Kasischke, N. H. F. French, and N. L. Christensen, "Sensitivity of ERS-1 and JERS-1 radar data to biomass and stand structure in Alaskan boreal forest," *Remote Sens. Environ.*, vol. 54, pp. 247–253, 1995.

[15] S. Englhart, V. Keuck, and F. Siegert, "Modelling aboveground biomass in tropical forests using multi-frequency SAR data—A comparison of methods," *IEEE J. Sel. Topics Appl. Earth Observ. Remote Sens.*, vol. 5, no. 1, pp. 298–306, Feb. 2012.

[16] T. Le Toan, A. Beaudoin, J. Riom, and D. Guyon, "Relating forest biomass to SAR data," *IEEE Trans. Geosci. Remote Sens.*, vol. 30, no. 2, pp. 403–411, Mar. 1992.

[17] T. Le Toan *et al.*, "The BIOMASS mission: Mapping global forest biomass to better understand the terrestrial carbon cycle," *Remote Sens. Environ.*, vol. 115, no. 11, pp. 2850–2860, 2011.

[18] P. Dubois-Fernandez *et al.*, "Forest biomass estimation from P-band high incidence angle data," in *Proc. POLINSAR 2005 Workshop*, Frascati, Italie, 6 pp [Online]. Available: http://earth.esa.int/workshops/polinsar 2005/participants/88/paper_Biomass_estimation_from_Pband.PDF

[19] C. Robinson, S. Saatchi, M. Neumann, and T. Gillespie, "Impacts of spatial variability on aboveground biomass estimation from L-band radar in a temperate forest," *Remote Sens.*, vol. 5, no. 3, pp. 1001–1023, 2013.

[20] R. Lucas *et al.*, "An evaluation of the ALOS PALSAR L-band backscatter-above ground biomass relationship Queensland, Australia: Impacts of surface moisture condition and vegetation structure," *IEEE J. Sel. Topics Appl. Earth Observ. Remote Sens.*, vol. 3, no. 4, pp. 576–593, Dec. 2010.

[21] S. T. Wu, "Potential application of multipolarization SAR for pine-plantation biomass estimation," *IEEE Trans. Geosci. Remote Sens.*, vol. GE-25, no. 3, pp. 403–409, May 1987.

[22] M. L. Imhoff, "A theoretical analysis of the effect of forest structure on synthetic aperture radar backscatter and the remote sensing of biomass," *IEEE Trans. Geosci. Remote Sens.*, vol. 33, no. 2, pp. 341–352, Mar. 1995.

[23] G. Sandberg, L. M. H. Ulander, J. E. S. Fransson, J. Holmgren, and T. Le Toan, "L- and P-band backscatter intensity for biomass retrieval in hemiboreal forest," *Remote Sens. Environ.*, vol. 115, pp. 2874–2886, 2011.

[24] A. Luckman, J. Baker, M. Honzák, and R. Lucas, "Tropical forest biomass density estimation using JERS-1 SAR: Seasonal variation, confidence limits, and application to image mosaics," *Remote Sens. Environ.*, vol. 63, pp. 126–139, 1998.

[25] I. H. Woodhouse, E. T. A. Mitchard, and C. M. Ryan, "Radar basckscatter is not a "direct measure" of forest biomass," *Nat. Clim. Change*, vol. 2, pp. 556–557, 2012.
[26] T. Castel, F. Guerra, Y. Caraglio, and F. Houllier, "Retrieval biomass of a large Venezuelan pine plantation using JERS-1 SAR data. Analysis of forest structure impact on radar signature," *Remote Sens. Environ.*, vol. 79, pp. 30–41, 2002.
[27] E. T. A. Mitchard *et al.*, "Using satellite radar backscatter to predict above-ground woody biomass: A consistent relationship across four different African landscapes," *Geophys. Res. Lett.*, vol. 36, p. L23401, 2009, doi: 23410.21029/22009GL040692.
[28] E. T. A. Mitchard *et al.*, "Measuring biomass changes due to woody encroachment and deforestation/degradation in a forest–savanna boundary region of central Africa using multi-temporal L-band radar backscatter," *Remote Sens. Environ.*, vol. 115, pp. 2861–2873, 2011.
[29] N. Floury, T. Le Toan, H. Jeanjean, A. Beaudoin, and O. Hamel, "L and C-band multipolarized backscatter responses of eucalyptus plantations in Congo," in *Proc. Geosci. Remote Sens. Symp. (IGARSS'95)*, 1995, vol. 1, pp. 728–730, doi: 10.1109/IGARSS.1995.520569.
[30] E. S. Kasischke, J. M. Melack, and M. Dobson, "The use of imaging radars for ecological applications—A review," *Remote Sens. Environ.*, vol. 59, pp. 141–156, 1997.
[31] R. M. Lucas and A. K. Milne, "Synthetic aperture radar for woodland biomass estimation in Australia: An overview," in *Proc. IEEE Int. Geosci. Remote Sens. Symp. (IGARSS'01)*, 2001, pp. 1421–1423.
[32] S. Englhart, V. Keuck, and F. Siegert, "Aboveground biomass retrieval in tropical forests—The potential of combined X- and L-band SAR data use," *Remote Sens. Environ.*, vol. 115, pp. 1260–1271, 2011.
[33] M. C. Dobson *et al.*, "Estimation of forest biophysical characteristics in northern Michigan with SIR-C/X-SAR," *IEEE Trans. Geosci. Remote Sens.*, vol. 33, no. 4, pp. 877–895, Jul. 1995.
[34] F. F. Gama, J. R. Dos Santos, and J. C. Mura, "Eucalyptus biomass and volume estimation using interferometric and polarimetric SAR data," *Remote Sens.*, vol. 2, pp. 939–956, 2010, doi: 10.3390/rs2040939.
[35] G. Le Maire *et al.*, "MODIS NDVI time-series allow the monitoring of Eucalyptus plantation biomass," *Remote Sens. Environ.*, vol. 115, no. 10, pp. 2613–2625, 2011.
[36] N. Baghdadi *et al.*, "Testing different methods of forest height and above-ground biomass estimations from ICESat/GLAS data on Eucalyptus plantations in Brazil," *IEEE J. Sel. Topics Appl. Earth Observ. Remote Sens.*, vol. 7, no. 1, pp. 290–299, Jan. 2014.
[37] J. Zhou *et al.*, "Mapping local density of young Eucalyptus plantations by individual tree detection in high spatial resolution satellite images," *Forest Ecol. Manage.*, vol. 301, pp. 129–141, 2013.
[38] C. Marsden *et al.*, "Modifying the G'DAY process-based model to simulate the spatial variability of Eucalyptus plantation growth on deep tropical soils," *Forest Ecol. Manage.*, vol. 301, pp. 112–128, 2013.
[39] G. Le Maire *et al.*, "Leaf area index estimation with MODIS reflectance time series and model inversion during full rotations of Eucalyptus plantations," *Remote Sens. Environ.*, vol. 115, pp. 586–599, 2011.
[40] C. Marsden *et al.*, "MODIS vegetation index time-series with structure, light absorption and stem production of fast-growing Eucalyptus plantations," *Forest Ecol. Manage.*, vol. 259, no. 9, pp. 1741–1753, 2010.
[41] A. Peregon and Y. Yamagata, "The use of ALOS/PALSAR backscatter to estimate above-ground forest biomass: A case study in Western Siberia," *Remote Sens. Environ.*, vol. 137, pp. 139–146, 2013.
[42] R. Avtar, R. Suzuki, W. Takeuchi, and H. Sawada, "PALSAR 50 m mosaic data basel national level biomass estimation in Cambodia for implementation of REDD& mechanism," *PLoS One*, vol. 8, pp. e74807, 2013.
[43] J. N. Collins *et al.*, "Estimating land-scape vegetation carbon stocks using airborne multi-frequency polarimetric synthetic aperture radar (SAR) in the savannahs of north Australia," *Int. J. Remote Sens.*, vol. 30, no. 5, pp. 1141–1159, 2009.
[44] M. A. Karam *et al.*, "A microwave polarimetric scattering model for forest canopies based on vector radiative transfer theory," *Remote Sens. Environ.*, vol. 53, pp. 16–30, 1995.
[45] C. Proisy, E. Mougin, F. Fromard, and M. A. Karam, "Interpretation of polarimetric radar signatures of mangrove forests," *Remote Sens. Environ.*, vol. 71, pp. 56–66, 2000.
[46] C. Proisy, E. Mougin, F. Fromard, V. Trichon, and M. A. Karam, "On the influence of canopy structure on the radar backscattering of mangrove forests," *Int. J. Remote Sens.*, vol. 23, no. 20, pp. 4197–4210, 2002.
[47] A. J. Luckman, J. Baker, R. Lucas, and T. M. Kuplich, "Retrieval of the biomass of regenerating tropical forest in Amazonia using spaceborne SAR data," in *Proc. Int. Symp. Retrieval Bio- Geophys. Parameters SAR Data L Appl.*, Toulouse, France, Oct. 1995, ESA SP-441. Noordwijk, The Netherlands: ESA, 1996, pp. 107–118.
[48] J. R. Santos, M. S. Pardi Lacruz, L. S. Araujo, and M. Keil, "Savanna and tropical rainforest biomass estimation and spatialization using JERS-1 data," *Int. J. Remote Sens.*, vol. 23, no. 7, pp. 1217–1229, 2002.
[49] L. Breiman, "Random forests," *Mach. Learn.*, vol. 45, no. 1, pp. 5–32, 2001.
[50] V. Rodriguez-Galiano, B. Ghimire, J. Rogan, M. Chica-Olmo, and J. Rigol-Sanchez, "An assessment of the effectiveness of a random forest classifier for land-cover classification," *ISPRS J. Photogramm. Remote Sens.*, vol. 67, pp. 93–104, 2012.
[51] M. A. Tanase *et al.*, "Airborne multi-temporal L-Band polarimetric SAR data for biomass estimation in semi-arid forests," *Remote Sens. Environ.*, vol. 145, pp. 93–104, 2014.
[52] A. T. Hudak *et al.*, "Quantifying aboveground forest carbon pools and fluxes from repeat LiDAR surveys," *Remote Sens. Environ.*, vol. 123, pp. 25–40, 2012.
[53] J. Mascaro *et al.*, "A tale of two "Forests": Random Forest machine learning aids tropical forest carbon mapping," *PLoS One*, vol. 9, no. 1, p. e85993, 2014.
[54] J. L. Stape *et al.*, "The Brazil Eucalyptus potential productivity project: Influence of water, nutrients and stand uniformity on wood production," *Forest Ecol. Manage.*, vol. 259, pp. 1686–1694, 2010.
[55] T. Le Toan *et al.*, "The BIOMASS mission: Mapping global forest biomass to better understand the terrestrial carbon cycle," *Remote Sens. Environ.*, vol. 115, pp. 2850–2860, 2011.

Nicolas N. Baghdadi received the Ph.D. degree from the University of Toulon, La Garde, France, in 1994.

From 1995 to 1997, he was a postdoctoral researcher at INRS ETE—Water Earth Environment Research Centre, Quebec University, QC, Canada. From 1998 to 2008, he was with French Geological Survey (BRGM), Orléans, France. Since 2008, he has been a Senior Scientist with the National Research Institute of Science and Technology for Environment and Agriculture (IRSTEA), Montpellier, France. His research interests include microwave remote sensing, image processing, analysis for satellite and airborne remote sensing data, analysis of SAR data, and the retrieval of soil parameters (surface roughness and moisture content).

Guerric Le Maire received the M.Sc. degree in agronomy, specialized in ecology, from the National Institute of Agronomy (INA P-G), Paris, France, in 2002, and the Ph.D. degree in plant ecophysiology from Paris XI University, Orsay, France, in 2005.

From 2006 to 2007, he did a Post-Doc with the Laboratoire des Sciences du Climat et de l'Environnement, Saclay, France, on regional modeling of forest growth. He joined the Cirad (French Agricultural Research Centre for International Development), Montpellier, France, in 2008. His research interests include remote-sensing image processing/analysis and process-based forest models development applied to tropical forest plantations.

Jean-Stéphane Bailly received the B.E. degree in agronomy, the M.Sc. degree in Biostatistics, and the Ph.D. degree in hydrology.

Since 1991, He has been a Member of the French Civil Corps of Water and Forestry Engineers. He is a Senior Lecturer and Scientist in Physical Geography with AgroParisTech, Montpellier, France. His research interests include spatial observations and parameterizations for hydrological modeling.

Kenji Osé is a GIS and Remote Sensing Engineer with UMR Tetis, IRSTEA, Montpellier, France. His research interests include responsible agriculture and territories sustainable planning using optical satellite imagery. He also contributes to Equipex GeoSud, a project dedicated to the acquisition and provision of satellite coverage of the entire French territory (images at different times with different sensors) with special attention given to urban areas.

Yann Nouvellon received the M.Sc. degree in agronomy from ENSAIA, Nancy, France, in 1994, and the Ph.D. degree in agronomy from the National Institute of Agronomy (INA P-G), Paris, France, in 1999.

From 1999 to 2000, he did a Post-Doc at USDA-ARS SWRC, Tucson, AZ, USA, to apply a spatially-explicit, hydro-ecological model over a semi-arid grassland watershed using remotely sensed data (Landsat imagery) and other spatially-distributed data (soil maps, meteorological data). He joined the French Agricultural Research Centre for International Development (CIRAD), Montpellier, France, in 2000. His research interests include carbon and water cycles and the ecophysiology of fast growing eucalypt plantations.

Mehrez Zribi received the B.E. degree in signal processing from the Ecole Nationale Supérieure d'Ingénieurs en Constructions Aéronautiques (ENSICA), Toulouse, France, and the Ph.D. degree from the Université Paul Sabatier, Toulouse, France.

In 1995, he joined the CETP Laboratory (IPSL/CNRS), Vélizy, France. He is employed by Centre National de Recherche Scientifique (CNRS), Paris, France, since 2001. In October 2008, he joined CESBIO Laboratory. His research interests include microwave remote sensing applied to hydrology and microwave modeling and instrumentations.

Cristiane Lemos received the Ph.D. degree in science forestry from the University of São Paulo, São Paulo, Brazil, in 2012.

Since 2010, She has been a Forestry Researcher with the International Paper. There, she has been working with empirical and ecophysiological modeling, remote sensing, silviculture, and management of *Eucalyptus* plantations. Her challenge is to monitor quality and productivity of *Eucalyptus* plantations using remote sensing techniques.

Rodrigo Hakamada was born in São Paulo state, Brazil, in 1981. He is currently pursuing the Ph.D. degree at the University of São Paulo, São Paulo, Brazil, studying water relationships in *Eucalyptus* plantations.

He has worked with forest researches since 2005, when he finished his undergraduate in Forest Engineering at the São Paulo University. The focus of his master thesis was to monitor forest plantations and silviculture operations using inventory data. His research interests include integration of silviculture, ecophisiology, and remote sensing techniques in forest plantations.